JOC The Journal of Organic Chemistry

Article

pubs.acs.org/joc

Synthesis of Eight-Arm, Branched Oligonucleotide Hybrids and Studies on the Limits of DNA-Driven Assembly

Alexander Schwenger, Claudia Gerlach, Helmut Griesser, and Clemens Richert*

Institute for Organic Chemistry, University of Stuttgart, 70569 Stuttgart, Germany

Supporting Information

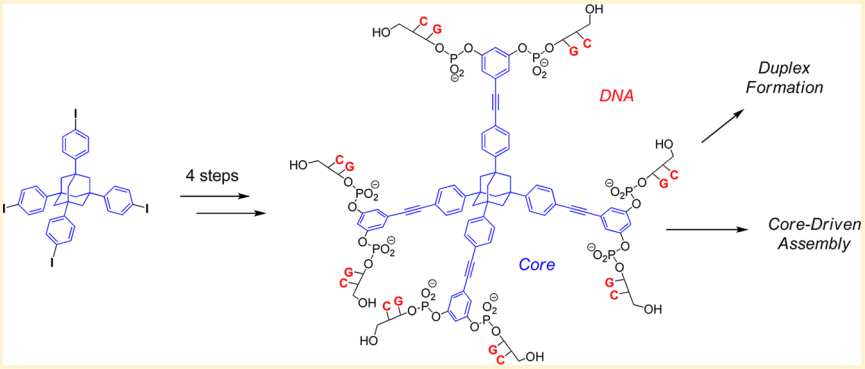

ABSTRACT: Oligonucleotide hybrids with organic cores as rigid branching elements and four or six CG dimer strands have been shown to form porous materials from dilute aqueous solution. In order to explore the limits of this form of DNA-driven assembly, we prepared hybrids with three or eight DNA arms via solution-phase syntheses, using *H*-phosphonates of protected dinucleoside phosphates. This included the synthesis of $(CG)_8$TREA, where TREA stands for the tetrakis[4-(resorcin-5-ylethynyl)phenyl]adamantane core. The ability of the new compounds to assemble in a DNA-driven fashion was studied by UV-melting analysis and NMR, using hybrids with self-complementary CG zipper arms or non-self-complementary TC dimer arms. The three-arm hybrid failed to form a material under conditions where four-arm hybrids did so. Further, the assembly of TREA hybrids appears to be dominated by hydrophobic interactions, not base pairing of the DNA arms. These results help in the design of materials forming by multivalent DNA−DNA interactions.

INTRODUCTION

Base pairing between complementary oligonucleotides is one of the most reliable forms of molecular recognition. Nature uses base pairing for the transmission of genetic information.[1,2] Duplex formation between complementary oligonucleotides can also be used to construct non-natural, designed nanostructures.[3−6] Further, oligonucleotide chains, when covalently appended to inorganic or organic branching elements, can serve as "sticky ends" whose hybridization with complementary sequences drives the formation of designed assemblies. Among the branching elements for which assembly has been demonstrated are gold nanoparticles[7−10] and organic tectons or cores.[11−15] This suggests that rule-based molecular recognition between nucleic strands operates beyond the realm of linear DNA and RNA duplexes.

We have recently described DNA hybrids consisting of a rigid organic branching element (or core) as preorganizing framework and short oligodeoxynucleotide arms as sticky ends that avoid the flexible linkers typically found in bioconjugates.[16,17] Complementary DNA arms were shown to drive the formation of nanoporous materials from dilute aqueous solutions upon addition of divalent cations. Hybrids with tetrakis(hydroxyphenyl)methane (TPM), hexakis(*p*-hydroxyphenyl)-*p*-xylene (HPX) (Figure 1), or tetrakis(*p*-triazoylphenyl)adamantane (TTPA) as core all gave materials when featuring CG dimers as sticky ends and did not produce materials with non-self-complementary TC dimers as DNA arms.[18] The temperature and salt concentration at which the materials form were found to depend strongly on the rigidity of the core, the number of like charges, and the number of DNA chains. Most recently, we reported solution-phase syntheses relying on phosphoramidite or *H*-phosphonate couplings that allow for the synthesis of larger quantities of the hybrids,[19,20] including the synthesis of hybrids with tetrakis(*p*-hydroxybiphenyl)adamantane (TBA) as core (Figure 1). Some materials formed from branched oligonucleotide hybrids have been shown to take up small molecules, including chromophores that are photoactive in the bound state.[18,20]

Previous studies showed that the number of DNA arms has a strong effect on the assembly properties, but the size and structure of the core are also important.[20] We wished to extend this work to hybrids with organic cores of even larger size, hoping to eventually produce materials that can take up and

Received: September 25, 2014
Published: November 19, 2014

dx.doi.org/10.1021/jo5022053 | J. Org. Chem. 2014, 79, 11558−11566

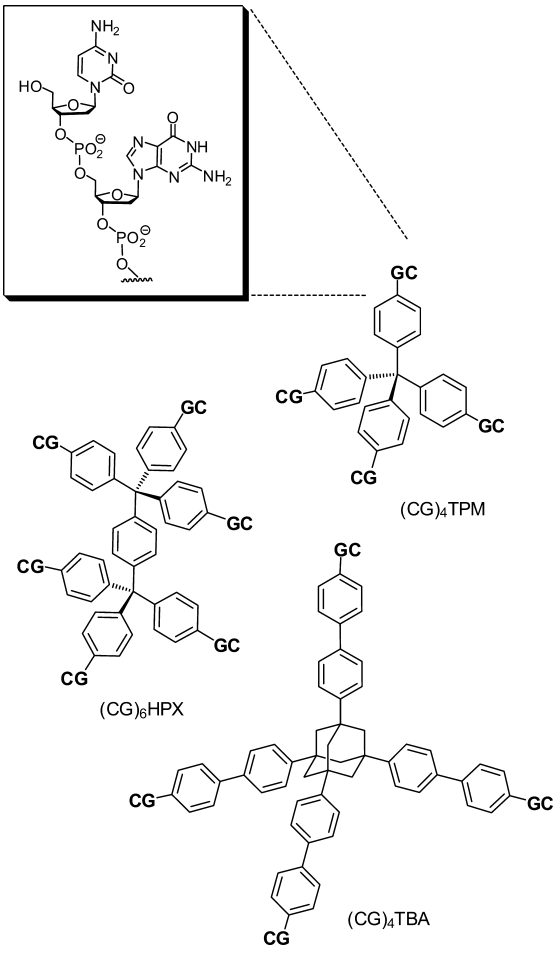

Figure 1. Structures of some known oligonucleotide hybrids.

release large guest molecules. Further, we wished to increase the number of DNA arms beyond 6, so as to increase the thermal stability of the assemblies. In doing so, we also wished to further improve our synthetic methodology by tackling dendrimer-like targets requiring ever more demanding simultaneous couplings. Finally, we wished to explore the limits of DNA-driven assembly, assuming that the aggregation of large, rigid, and hydrophobic core structures would eventually dominate the intermolecular interactions of hybrids.

Here we report the solution-phase synthesis of two eight-arm DNA hybrids with tetrakis[4-(resorcinylethynyl)phenyl]-adamantane (TREA) as the core, including a hybrid with non-self-complementary DNA arms, two hybrids with eight arms lacking the ethynyl spacer, based on tetrakis(4-resorcinylphenyl)adamantane (TRPA) as the core, and two hybrids featuring trihydroxytriptycene (THT) as core, resulting in hybrids with just three DNA arms. The propensity of either of the hybrids to form higher order assemblies in aqueous buffer was monitored by UV-melting analysis and, in some instances, by ^{1}H NMR. We found that three CG arms do not suffice to induce the formation of a material with THT cores at micromolar concentrations, whereas the strong tendency of hybrids with a TREA core to assemble is driven, at least in part, by hydrophobic interactions between cores, not just duplex formation between DNA arms. The hybrids whose synthesis is presented here thus help to define the limits of DNA-driven assembly that can be induced by CG dimer arms as zippers.

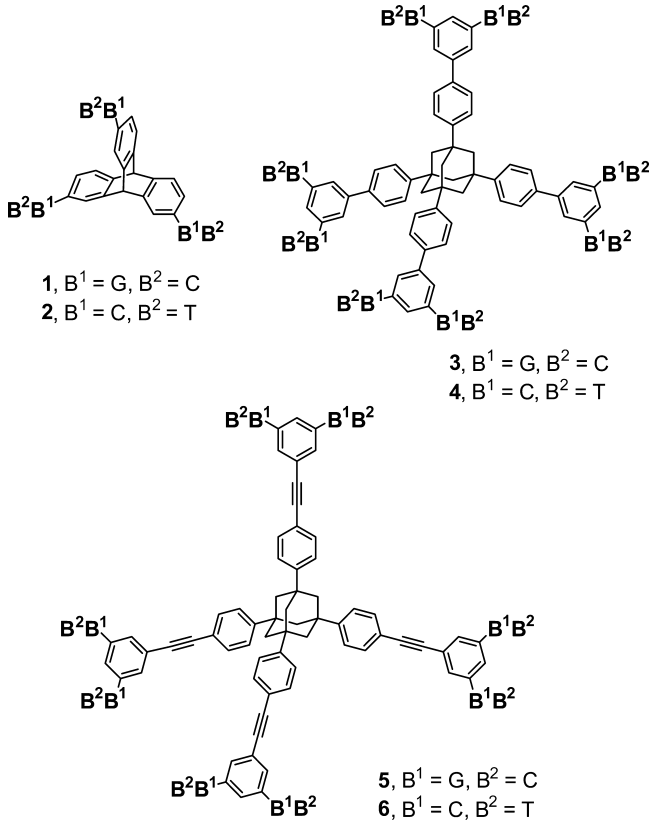

Figure 2. Structures of the target molecules of this study.

RESULTS AND DISCUSSION

Oligonucleotide hybrids with four or six DNA arms were studied in detail earlier.[17−20] As mentioned above, we wished to explore the limits of the multivalency-driven assembly process of such branched constructs by studying hybrids with just three DNA arms and with as many as eight DNA arms. Figure 2 shows the target molecules of this study. The first two of the hybrids, namely $(CG)_3$THT (**1**) and $(TC)_3$THT (**2**), are based on triptycene and feature three DNA arms. The second set, $(CG)_8$TRPA (**3**) and $(TC)_8$TRPA (**4**), has eight DNA arms, and so do the full-size hybrids $(CG)_8$TREA (**5**) and $(TC)_8$TREA (**6**), which have a longer linker with an ethynyl spacer. Either set of hybrids included one compound with self-complementary arms and one with non-self-complementary DNA sequences, so as to test for rule-based assembly.

The synthesis of **1** and **2** started from 2,7,14-trihydroxytriptycene (THT, **7**).[21] Syntheses of 2,6,14- and 2,7,14-trisubstituted triptycene derivatives are known from the literature. Other triply substituted triptycene are of interest for pharmaceutical applications,[22] supramolecular chemistry,[23] and materials sciences.[24] The dimer arms were installed using *H*-phosphonate solution-phase methodology[19] (Scheme 1). Specifically, coupling of *H*-phosphonate **8** or **9** to **7** produced a phosphite diester intermediate that was oxidized with iodine in pyridine/water, detritylated with dichloroacetic acid, and finally converted to fully deprotected **1** and **2** through treatment with aqueous ammonia. The entire reaction sequence from **7** to **1** or **2** was performed without purification of intermediates and gave the three-arm hybrid **1** in 60% overall yield after cartridge purification. The overall yield of **2** was 40% under similar conditions.

dx.doi.org/10.1021/jo5022053 | J. Org. Chem. 2014, 79, 11558−11566

Scheme 1

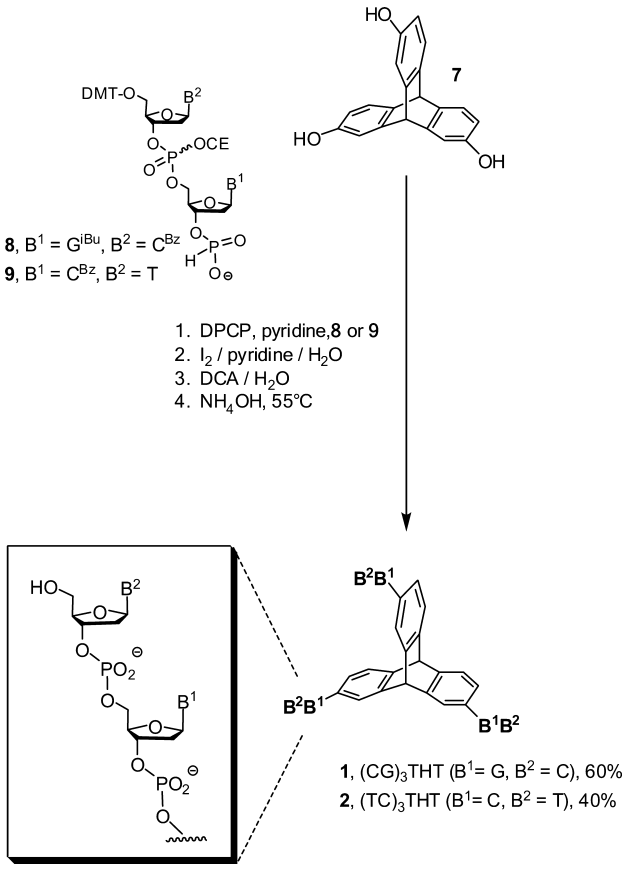

The octaols serving as cores for eight-arm hybrids **3**–**6** were accessible from 1,3,5,7-tetrakis(4-iodophenyl)adamantane (**10**), which is known to be accessible from bromoadamantane in two steps via a Friedel–Crafts reaction and iodination.[25–27] The route to tetrakis(4-resorcinylphenyl)adamantane (TRPA, **11**) started with a Suzuki reaction involving 3,5-dimethoxyphenylboronic acid, whereas the elaboration of tetrakis[4-(resorcin-5-ylethynyl)phenyl]adamatane (TREA, **12**) started with a Sonogashira coupling between **10** and 1-ethynyl-3,5-dimethoxybenzene (Scheme 2).

To avoid crippling yields in the first step of the synthesis of dendrimer-like **12**, different educts and reaction conditions were tested. In the initial screen for the 4-fold Sonogashira reaction (not shown in Scheme 2) 1-iodo-3,5-dimethoxybenzene and tetrakis(4-ethynylphenyl)adamantane[18–20] were employed, using solvent/base combinations, such as toluene/diethylamine, neat diethylamine, toluene/triethylamine, TBAF/THF, neat triethylamine, and DMF/diethylamine. A screen of Pd/Cu catalyst ratios, as well as different temperatures and reaction times, was also performed. With neat triethylamine as solvent, a catalyst ratio of 1.0/1.9 (Pd/Cu), a reaction temperature of 80 °C, and a reaction time of 3–4 days, a yield of 26% of octaether **13** or 71% per arm was achieved. With tetraiodide **10** as halide, 1-ethynyl-3,5-dimethoxybenzene as alkyne, a catalyst ratio of 1/1.6 (Pd/Cu), 80 °C, and a reaction time of 12 h, a yield of 57% of **13** or 87% per linker arm coupling was obtained. Subsequent 8-fold ether cleavage with BBr_3 then gave **12** in near-quantitative yield, resulting in an overall yield of 56% over 2 steps. The 4-fold Suzuki reaction gave octaether **14** in 36% yield under conventional conditions (0.04 equiv of $Pd(PPh_3)$, K_2CO_3, 100 °C) and was not optimized further. Demethylation of **14** gave the desired octaol **11** in 94% yield, so that an overall yield of 35% over two steps resulted for this core.

We then assembled DNA hybrids **3** and **4** (Scheme 3) using *H*-phosphonate chemistry and the general approach described for **1** and **2**, above. It was challenging to achieve near-complete 8-fold coupling, and an extension of the reaction time proved the most important step for overcoming this challenge. In the

Scheme 3

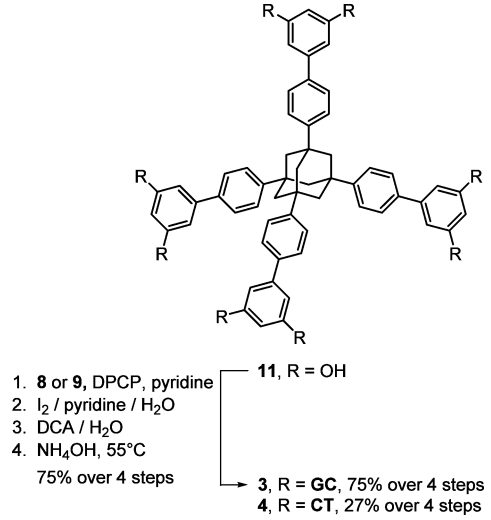

Scheme 2

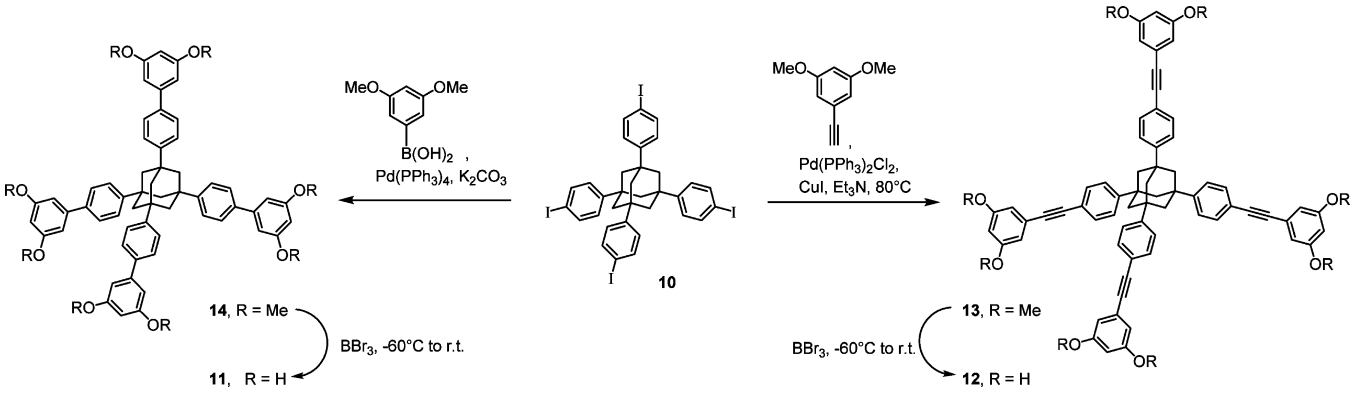

dx.doi.org/10.1021/jo5022053 | J. Org. Chem. 2014, 79, 11558–11566

optimized protocol, 3.5 equiv of dimer *H*-phosphonate (**8** or **9**) per phenolic group were employed in the coupling, with a mixture of pyridine and CH_3CN (4/1, v/v) as solvent and diphenyl chlorophosphate (DPCP) as condensing agent for 2 h at −40 °C, followed by oxidation with aqueous iodine in pyridine. After aqueous workup, detritylation and aminolysis were performed analogously to earlier hybrid syntheses.[19] Only after all protecting groups had been removed did MALDI-TOF mass spectra of crudes show product peaks of sufficient intensity under the matrix conditions tested. With the optimized protocol, hardly any hybrids lacking DNA arms were observed in those spectra, and no more than the expected intensities of symmetrical pyrophosphate, presumably formed from **8** or **9** during the course of the coupling reaction.

Scheme 4 shows the syntheses of the largest eight-arm hybrids (**5** and **6**), which started from **12** as core. As for the other two cores, *H*-phosphonate dimers **8** and **9** were employed. Either dimer gave slightly less conversion than for **11** in the coupling step, though respectable yields of the final hybrids were obtained, given that 8-fold reactions had to be performed.

Scheme 4

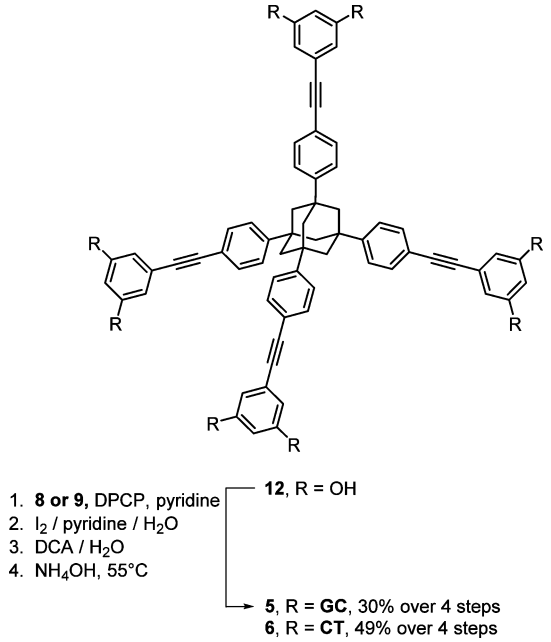

For either of the three eight-arm hybrids, a modest level of purity can be achieved by precipitation through slow diffusion of ethanol or methanol into an aqueous solution of the crude product. For TRPA-based **3** and **4**, pure hybrid was obtained by cartridge purification, using a step gradient of acetonitrile in water, after loading with a 50 mM ammonium acetate buffer. Up to 200 mg of crude product were purified to homogeneity per run on 10 g of stationary phase (C18). A large-scale synthesis of **3** (12 μmol) gave 50 mg of pure eight-arm hybrid (75% overall yield of isolated pure material). The purity was confirmed by analytical HPLC on a C-18 column at 55 °C and MALDI-TOF MS (see Figures S12 and S15, Supporting Information).

The purification of TREA-based hybrids **5** and **6** proved more challenging. Cartridge purification under conditions analogous to those used for **1**−**4** showed an unusually broad elution profile. Consequently, HPLC was employed. Here, an interesting phenomenon was observed for TREA hybrid **5**. Even with a slow gradient of acetonitrile at elevated temperature, a series of sharp peaks (marked with asterisks in Figure 3) was detected at retention times typical for hybrids.

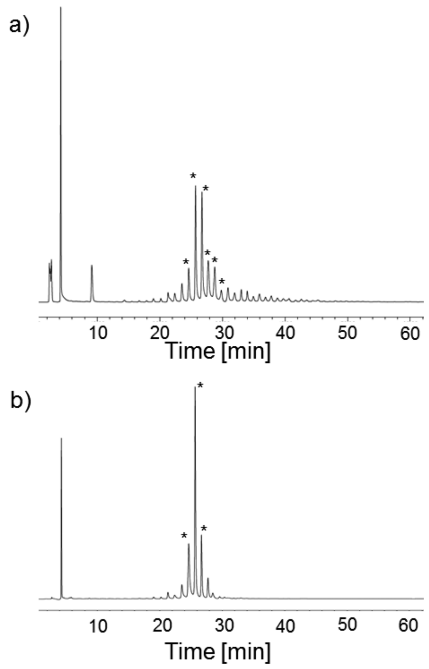

Figure 3. HPLC chromatograms of $(CG)_8$TREA (**5**) at 55 °C: (a) injection of crude product; (b) reinjection of the material from the most intense peak in (a). Conditions: C18-phase, gradient of 15−25% CH_3CN in 10 mM TEAA buffer, λ_{det} 260 nm.

Either of those peaks showed the correct mass for hybrid **5**. Reinjection of the material from the most prominent peak again gave a series of sharp peaks (Figure 3b), consistent with the hypothesis that the additional peaks were not caused by impurities but by different states of the same molecule. An increase in the column temperature during HPLC gave a more narrow distribution, again suggesting aggregation. Since the HPLC conditions chosen were denaturing for DNA duplexes (≥20% CH_3CN and ≥55 °C), this suggested that aggregates of the hybrid were present whose assembly was not driven by duplex formation between CG zipper arms. Instead, it appeared likely that a formation of oligomers was induced by hydrophobic interactions between the cores. This assumption was further confirmed when control hybrid **6** with non-self-complementary TC arms was subjected to the same HPLC conditions. Again, a series of peaks was detected with a similar, but slightly more narrow, peak distribution (Figure S10, Supporting Information).

We then proceeded to studying assembly processes by UV-melting analysis. For this, samples were first denatured in 0.01 M NaOH at 90 °C, neutralized in the heat, followed by cooling to 5 °C at a rate of 0.5 °C/min and subsequent heating to obtain a true melting curve at the same rate of 0.5 °C/min. The cooling and heating curves for hybrids **1**−**6** are shown in Figure 4. Additional melting curves under low salt conditions are shown in the Supporting Information. At 10 μM concentration, hybrid **1** with just three CG arms did not show any signs of assembly/melting, even at 100 mM $MgCl_2$. The smaller of the eight-arm hybrids with self-complementary arms (**3**) showed a

dx.doi.org/10.1021/jo5022053 | J. Org. Chem. 2014, 79, 11558−11566

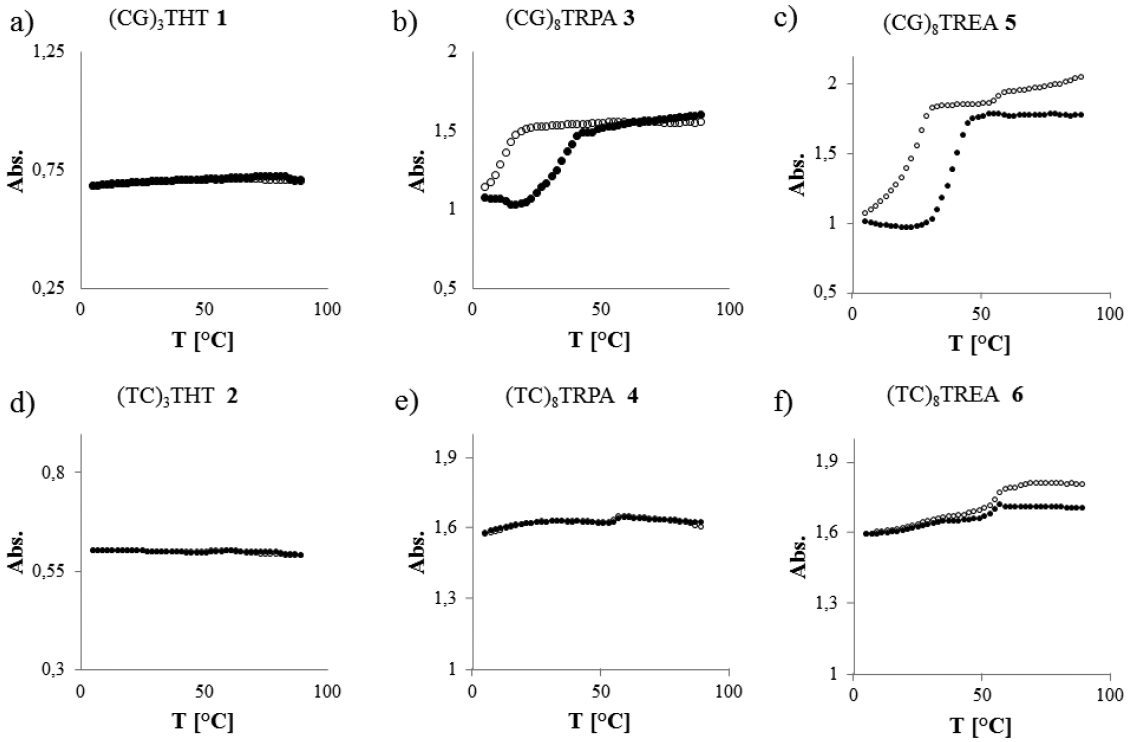

Figure 4. UV-melting profiles for DNA hybrids **1**−**6** measured at 10 μM hybrid concentration, 10 mM TEAA buffer, pH 7.0 plus 150 mM NaCl and 100 mM $MgCl_2$, as detected at 260 nm: (open circles) cooling curve; (filled circles) heating curve. The hybrids were first denatured in 10 mM NaOH at 90 °C, and the experiments were started by neutralizing with AcOH, analogously to experiments described earlier.[18,19] (For additional data, see Table S1, Supporting Information).

strong transition that was accompanied by visible turbidity, suggesting that part of the hybrid was forming a material. The assembly process was strongly salt-dependent, and no precipitation was observed in the absence of NaCl/$MgCl_2$ (see Figure S21, Supporting Information). During the subsequent heating of the high-salt sample, the assemblies melted again, but the resulting curve was shifted to higher temperatures in comparison to the cooling curve, as expected for larger aggregates that are slow to form and also break up more slowly than linear duplexes of unbranched oligonucleotides. The hysteresis between the heating and cooling curves is typical for hybrids with CG zippers,[19] and so is the large apparent hyperchromicity (which is, in fact, a combination of true hyperchromicity and the increase in concentration when the hybrid material dissolves again). For TRPA hybrid **4** with its TC arms, a minimal transition was observed that is too small to be explained by duplex formation between its arms.

Hybrid $(CG)_8$TREA (**5**) with its more extended core showed a broad and reversible transition in the melting experiment, even in the absence of NaCl/$MgCl_2$, with little hyperchromicity (Figure S23, Supporting Information). Upon addition of 150 mM NaCl alone, a modest hysteresis between cooling and heating curve appeared (Figure S24, Supporting Information). Addition of $MgCl_2$ then led to a hyperchromicity beyond what can reasonably be explained by duplex formation (Figure 4c), and the cloudiness of the sample indicated precipitation of insoluble material. Again, the transitions were reversible, with hysteresis between the cooling and heating curves.

Unlike control hybrids with non-self-complementary DNA arms studied earlier,[18−20] $(TC)_8$TREA (**6**) did show a transition in the UV-monitored cooling/heating experiment that was accompanied by significant hyperchromicity, both under low-salt conditions and in the presence of NaCl/$MgCl_2$ (16% in the latter case, Figure 4f). The temperature at which the transition occurred was similar to that found for the transitions of **5**, again suggesting that assembly independent of base pairing was occurring. The hyperchromicity was more modest than in the case of **3**, and little to no precipitation was observed at this hybrid concentration (10 μM), indicating that **6** lacks the strong tendency of **5** to self-aggregate through its DNA arms.

Next, we performed exploratory NMR experiments to better understand the aggregation behavior of the new branched hybrids. For this, 1 mM solutions of **1**, **5**, and **6** were measured under three different conditions: neutral pH and room temperature, neutral pH and 80 °C, and strongly basic pH (0.1 M NaOD) at 20 °C. Peaks assignments were confirmed via two-dimensional spectra of the same solutions (TOCSY). For the three-arm hybrid **1**, a modest level of peak broadening was observed in neutral solution at room temperature (Figure 5), suggesting that some assembly occurred at this hybrid concentration (which is 2 orders of magnitude higher than the concentration in the UV-monitored melting experiments). Heating to 80 °C then led to much sharper signals, indicating that what assemblies there were, were all but broken up.

For eight-arm hybrid **5** with its extended lipophilic core, extremely broad signals were observed in neutral D_2O solution at 20 °C (Figure 6). When the temperature was increased, a sharpening of all resonances was observed, but even under strongly basic conditions (that lead to full denaturation of linear DNA duplexes), line widths did not shrink sufficiently to show the triplets typical for the H1′ signals of nucleotides in DNA of similar molecular weight. Control hybrid **6** with its non-self-complementary TC arms behaved similarly to **5**, in that heating

dx.doi.org/10.1021/jo5022053 | J. Org. Chem. 2014, 79, 11558−11566

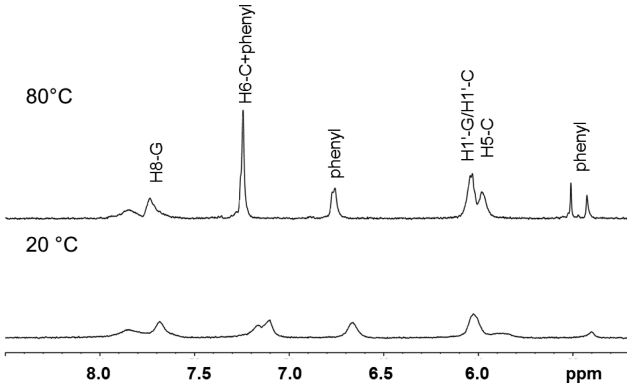

Figure 5. Low-field region of ^{1}H NMR spectra of $(CG)_3$THT (**1**) in D_2O with 10 mM phosphate buffer at 20 °C (bottom spectrum) and 80 °C (top spectrum) at 1 μM hybrid concentration and 500 MHz.

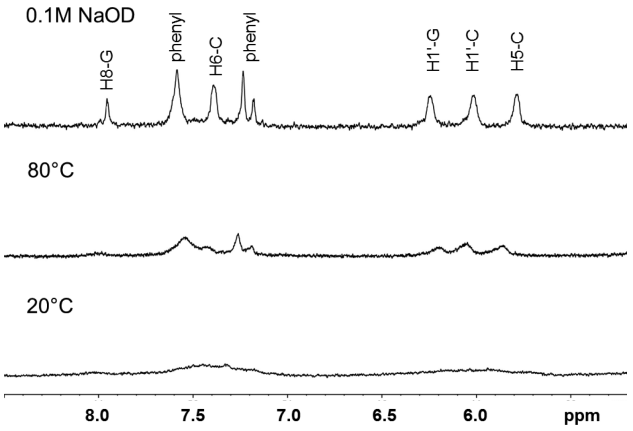

Figure 6. ^{1}H NMR spectra of $(CG)_8$TREA (**5**) in D_2O at 500 MHz in phosphate buffer (10 mM, pH 7) at 20 °C (bottom), at 80 °C (middle), or in 0.1 M NaOD at 20 °C (top). Note that the signal intensity for H8 of G decreases in strongly basic solution, most probably because of partial exchange for deuterium.

to 80 °C in neutral solution did not suffice to break up the aggregates that manifested themselves in broad signals (Figure 7). The extent of the broadening was weaker, though, than for **5**, again suggesting that the CG dimers of **5** contributed to the strong tendency to assemble into larger aggregates. Still, the

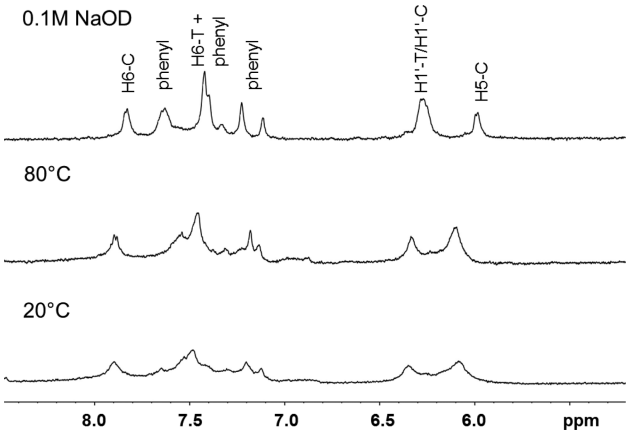

Figure 7. ^{1}H NMR spectra of $(TC)_8$TREA (**6**) in D_2O, 500 MHz in phosphate buffer (10 mM, pH 7) at 20 °C (bottom), at 80 °C (middle), or in 0.1 M NaOD at 20 °C (top).

stiff, extended, and lipophilic core apparently makes a very significant contribution, which is difficult to suppress, even if the overall number of negative charges is increased by deprotonating the G or T residues of the DNA arms.

Finally, we asked how the self-assembly of DNA hybrids such as **5**, which is still affected but no longer dominated by the DNA arms, might be driven by its lipophilic core. For this, we crystallized the methyl-protected TREA molecule **13**. Figure 8

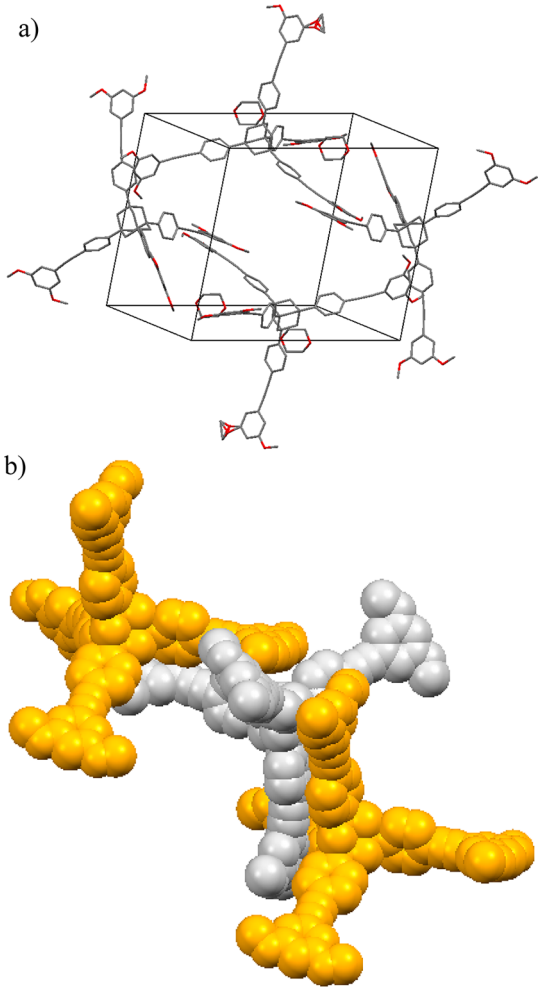

Figure 8. X-ray crystal structure of the $(Me)_8$TREA (**13**): (a) view showing the unit cell. Note that some methoxy groups were found to be disordered. (b) Expansion showing the packing of three molecules, with molecules shown in yellow being symmetrically equivalent.

shows the X-ray crystal structure obtained. In the crystal, individual molecules form an interpentrating network with strong interactions between phenyl moieties of linker arms, whose stacking distances are within the range typical for aromatic rings (≤3.5 Å). Though an identical arrangement is unrealistic for DNA-bearing derivatives, this suggests that, with hydrophobic extensions of this size and geometry, core-to-core interactions may compete with the predominantly DNA-driven assembly paths, resulting in hybrids no longer obeying base pairing rules alone.

CONCLUSIONS AND OUTLOOK

The results presented here show how the synthesis of branched oligonucleotides can be successfully expanded beyond the six-arm hybrids published earlier. Our results show that hybrids

dx.doi.org/10.1021/jo5022053 | J. Org. Chem. 2014, 79, 11558−11566

with eight short oligonucleotide arms can be prepared in monodisperse form using solution-phase synthesis. Despite this challenging level of branching, labile phenolic phosphodiester linkages,[20] and the steric crowding induced by the dendrimer-like structure, the *H*-phosphonate methodology proved reliable.

The current results also show that, for oligonucleotide hybrids whose size is between that of conventional hybridization probes and colloids statistically coated with DNA arms,[8] not all constructs obey the Watson/Crick base pairing rules. For $(CG)_3$THT with its three-arm structure, no assembly was observed at micromolar concentrations. With biphenyl linkers on an adamantane core, as in $(CG)_8$TRPA, properties similar to those found for tetrahedral hybrids with the same linker[19] were found. When expanding the length of the linkers to a diphenylacetylene unit, as in the TREA hybrids, assembly properties emerged that cannot be explained by Watson−Crick base pairing alone. The minimal number of DNA arms that leads to the formation porous materials thus appears to be 4.[17−19] Further, a shape ensuring that hydrophilic DNA arms shield the lipophilic core, so as to prevent hydrophobic interactions between cores, appears to be necessary, at least for eight-arm hybrids. A favorable balance between the number of CG zipper arms that induce DNA-driven, multivalent assembly and the hydrophobic interactions between large cores is lost for compounds such as **5**. Thus, the limits of rule-based interactions between branched DNA hybrids are now better defined.

EXPERIMENTAL SECTION

1,3,5,7-Tetrakis[3′,5′-dimethoxy-(1,1′-biphenyl)-4-yl]-adamantane (14). In a two-neck, round-bottom flask equipped with a condenser and magnetic stirrer were placed 1,3,5,7-tetrakis(4-iodophenyl)adamantane (**10**; 100 mg, 0.11 mmol, 1 equiv), toluene (3 mL), and $Pd(PPh_3)_4$ (5 mg, 0.004 mmol, 0.04 equiv) under nitrogen. When the solids had dissolved, K_2CO_3 (0.75 mL of 2 M aqueous solution) was added, followed by 3,5-dimethoxyphenylboronic acid (84 mg, 0.45 mmol, 4.3 equiv, in 0.75 mL of ethanol). The mixture was heated at reflux under nitrogen for 12 h. After the mixture was cooled to room temperature, H_2O_2 (30%, 0.5 mL) was added. The mixture was then stirred for 1 h. Toluene (10 mL) and water (10 mL) were added, and the layers were separated. The organic layer was dried over Na_2SO_4 and evaporated to dryness in vacuo. Purification via column chromatography (silica gel, 20 g, petroleum ether/CH_2Cl_2, 1/2 to 1/3, v/v) yielded 38 mg (0.04 mmol, 37%) of **14** as a colorless solid: R_f = 0.3 (petroleum ether/CH_2Cl_2 1/3, v/v); ^{1}H NMR (300 MHz, $CDCl_3$) δ 2.27 (s, 12 H), 3.84 (s, 24 H), 6.46 (t, ^4J = 2.2 Hz, 4 H), 6.74 (d, ^4J = 2.2 Hz, 8 H), 7.58 (s, 16 H); ^{13}C NMR (75.5 MHz, $CDCl_3$) δ 39.2, 47.3, 55.4, 99.1, 105.4, 125.4, 127.1, 139.1, 143.1, 148.7, 161.0 ppm; MS (FAB, 3-NBA) *m*/*z* (%) 987 (23) $[M + 3H]^+$, 986 (64) $[M + 2H]^+$, 985 (100) $[M + H]^+$, 984 (46) $[M]^+$; HRMS (ESI-TOF) *m*/*z* calcd for $C_{66}H_{64}O_8$ $[M + H]^+$ 984.460, *m*/*z* obsd 984.460.

1,3,5,7-Tetrakis{4-[(3,5-dimethoxyphenyl)ethynyl]phenyl}-adamantane (13). In a flask fitted with a condenser and magnetic stirrer were placed 1,3,5,7-tetrakis(4-iodophenyl)adamantane (**10**; 350 mg, 0.35 mmol, 1 equiv), 1-ethynyl-3,5-dimethoxybenzene (467.6 mg, 2.88 mmol, 8.19 equiv), $PdCl_2(PPh_3)_2$ (7.4 mg, 0.01 mmol, 0.03 equiv), CuI (3.4 mg, 0.018 mmol, 0.05 equiv), and a solvent mixture consisting of NMP (3.9 mL) and NEt_3 (1.9 mL) under argon. The mixture was heated to 80 °C under a static argon atmosphere for 8 h. Afterward, the reaction mixture was taken up in $CHCl_3$ (40 mL), extracted with water (50 mL), and washed with brine (50 mL). The organic layer was separated, dried over $MgSO_4$, and evaporated to dryness in vacuo. The residue was dissolved in CH_2Cl_2 (5 mL) and precipitated with CH_3OH (40 mL). After centrifugation (3500 rpm, 5 min) the supernatant was aspired. This procedure was repeated once. The precipitate was dried in vacuo. Purification via column chromatography (silica gel, 30 g, petroleum ether/CH_2Cl_2 1/3, v/v) yielded 211 mg (0.2 mmol, 57%) of **13** as a colorless solid: R_f = 0.25 (petroleum ether/CH_2Cl_2 1/2, v/v); ^{1}H NMR (300 MHz, $CDCl_3$) δ 2.17 (s, 12H), 3.80 (s, 24 H), 6.46 (t, ^4J = 2.2 Hz, 4 H), 6.69 (d, ^3J = 2.2 Hz, 8 H), 7.47 (d, ^3J = 8.6 Hz, 8 H), 7.54 (d, ^3J = 8.6 Hz, 8 H); ^{13}C NMR (75.5 MHz, $CDCl_3$) δ 39.3, 46.8, 55.4, 88.8, 89.2, 101.8, 109.3, 121.0, 124.5, 125.1, 131.7, 149.2, 160.5 ppm; HRMS (ESI-TOF) *m*/*z* calcd for $C_{74}H_{64}O_8$ 1081.467, *m*/*z* obsd 1081.468.

General Protocol A (Demethylation). In a dry flask were placed a solution of BBr_3 (2.5 equiv per OMe group of core) and $CHCl_3$ or CH_2Cl_2 (3 mL) under argon. After the mixture was cooled to −60 °C, a solution of and **13** or **14** (0.13 mmol) in $CHCl_3$ or CH_2Cl_2 (4.5 mL) was added dropwise (exothermic reaction). The mixture was stirred for an additional 3 h at this temperature followed by 19 h at room temperature, while a precipitate appeared. The mixture was then treated with CH_3OH (3 × 10 mL) and dried in vacuo.

1,3,5,7-Tetrakis[4-(resorcin-5-ylethynyl)phenyl]adamatane (12). The reaction was performed following general protocol A, starting from 1,3,5,7-tetrakis{4-[(3,5-dimethoxyphenyl)ethynyl]phenyl}-adamantane (**13**; 145 mg, 134 μmol) to yield 128 mg (132 μmol, quantitative) of **13** as a light brown solid: R_f = 0.27 (CH_2Cl_2/CH_3OH 6/1, v/v); ^{1}H NMR (300 MHz, CD_3OD) δ 2.12 (s, 12 H), 6.26 (t, ^4J = 2.2 Hz, 4 H), 6.41 (d, ^3J = 2.2 Hz, 8 H), 7.45 (d, ^3J = 8.6 Hz, 8 H), 7.51 (d, ^3J = 8.6 Hz, 8 H); ^{13}C NMR (75.5 MHz, CD_3OD) δ 40.6, 47.9, 55.4, 88.9, 90.5, 105.0, 110.9, 122.4, 125.6, 126.5, 132.6, 151.0, 160.2 ppm; HRMS (ESI-TOF) *m*/*z* calcd for $C_{66}H_{48}O_8$ 968.334, *m*/*z* obsd 968.334.

1,3,5,7-Tetrakis(p-resorcinylphenyl)adamantane (11). The reaction was performed following general protocol A, starting from 1,3,5,7-tetrakis[3′,5′-dimethoxy-(1,1′-biphenyl)-4-yl]adamantane (**14**; 27.5 mg, 28 μmol) to yield 23 mg (26 μmol, 94%) of **11** as a light brown solid: R_f = 0.27 (CH_2Cl_2/CH_3OH 6/1, v/v); ^{1}H NMR (300 MHz, CD_3OD) δ 2.01 (s, 12 H), 6.18 (t, ^4J = 2.1 Hz, 4 H), 6.5 (d, ^3J = 2.1 Hz, 8 H), 7.37 (d, ^3J = 8.5 Hz, 8 H), 7.44 (d, ^3J = 8.5 Hz, 8 H). ^{13}C NMR (75.5 MHz, CD_3OD) δ 40.3, 102.4, 106.5, 126.5, 127.8, 140.1, 144.4, 150.2, 159.9 ppm; HRMS (ESI-TOF) *m*/*z* calcd for $C_{58}H_{48}O_8$ 871.327, *m*/*z* obsd 871.325.

General Protocol B (Assembly of DNA Hybrids). A sample of the core (5−20 μmol, **7**, **11**, or **12**) was dried for 1 h at 85 °C and 0.001 mbar and then mixed with *H*-phosphonate dimer (**8** or **9**, 2.5−3.5 equiv per phenolic group of the core). After addition of molecular sieves 3 Å (five to seven beads), the mixture was dried again for 1−2 h at 40 °C and 0.001 mbar. The flask was flushed with argon and sealed with a septum, and a mixture of dry pyridine and CH_3CN (0.5−2.5 mL, 4/1, v/v) was added. After the mixture was cooled to −40 °C, diphenyl chlorophosphate (DPCP, 1.5 equiv to dimer) was added, and this mixture was stirred for 60−120 min at −40 °C. Then, a solution of iodine in dry pyridine (1 M, 1.5 equiv to dimer) was added, followed by H_2O (5 equiv) after 1−2 min. The reaction mixture was stirred for 10 min at −40 °C and then for 30 min at room temperature. After addition of CH_2Cl_2 (10 mL), the mixture was washed with a solution of aqueous sodium thiosulfate (7 mL, 10%, w/w) and aqueous phosphate buffer (5 mL, 0.2 M, pH 7). The aqueous phase was separated and back-extracted with CH_2Cl_2 three times (3 × 5 mL). The combined organic layers were concentrated in vacuo. The residue was coevaporated twice from toluene and dissolved in a minimal amount of CH_2Cl_2 (approximately 5 mL), followed by precipitation with MTBE (20 mL) and centrifugation (3500 rpm, 5 min). This procedure was repeated twice. The residue was then dissolved in CH_2Cl_2 (5 mL) and separated from the remaining solid, which was washed twice with CH_2Cl_2 (2 mL). The combined organic layers were concentrated in vacuo to yield the crude, fully protected hybrid, which was deprotected without further purification. For removal of the DMT groups, the protected hybrid was dissolved in CH_2Cl_2 (10 mL) and H_2O (10 equiv), followed by addition of dichloroacetic acid (DCA, 6% in CH_2Cl_2, 10 mL, 3.5 mmol). After 15 min, the reaction was quenched by addition of CH_3OH (4 mL). The solution was then concentrated, and the hybrid was precipitated by addition of MTBE (15 mL). The precipitate was separated by centrifugation, redissolved in a minimal volume of CH_2Cl_2/CH_3OH (1−4 mL, 9/1, v/v), and

dx.doi.org/10.1021/jo5022053 | J. Org. Chem. 2014, 79, 11558−11566

precipitated again by addition of MTBE (15 mL). This process was repeated two more times to give the crude DMT-deprotected hybrid. Cyanoethyl groups and the protecting groups of the nucleobases were removed by treating the crude product with ammonium hydroxide (25%, 5 mL) for 5 h at 55 °C. Excess ammonia was removed by passing a stream of N_2 over the surface until the sample was odorless. The remaining solution was evaporated to dryness by lyophilization to yield the crude hybrid (**1**–**6**). The crude product was then purified by reversed-phase HPLC (C8 column) using a gradient of 5–40% CH_3CN in 10 mM TEAA buffer at 55 °C or by Sep-Pak C_{18} cartridge purification, using a gradient of 0–20% CH_3CN in 10 mM NH_4Ac buffer.

*(CG)$_3$THT (**1**).* General protocol B was employed, starting from THT core **7** (1.2 mg, 4 μmol) and **8** (41 mg, 36 μmol) in pyridine and CH_3CN (0.5 mL, 4/1, v/v) for 1 h at −40 °C. After full deprotection, a portion of the crude hybrid was dissolved in 10 mM TEAA buffer containing 5% CH_3CN and subjected to HPLC purification (C18 column, 250 × 20 mm), using a gradient of CH_3CN in 10 mM TEAA buffer, 5–30% in 60 min at 55 °C. Hybrid **1** eluted at t_R = 16.0 min. The remaining crude hybrid was dissolved in 100 mM NH_4Ac buffer and subjected to cartridge purification (C18 column, Vac 35 cm^3), using a gradient of CH_3CN in 10 mM NH_4Ac buffer, 0–20%. Hybrid **1** eluted at 7.5%, yield 5.5 mg (2.4 μmol, 60%): MALDI-TOF-MS *m/z* calcd for $C_{77}H_{86}N_{24}O_{39}P_6$ $[M - H]^-$ 2156, *m/z* obsd 2156.

*(TC)$_3$THT (**2**).* The hybrid was prepared following general protocol B, starting from THT core **7** (2.6 mg, 8.6 μmol) and **9** (100 mg, 95 μmol) in pyridine and CH_3CN (1.5 mL, 4/1, v/v) for 2 h at −40 °C. HPLC purification (C18 column) using a gradient of CH_3CN in 10 mM TEAA buffer, 1–35% in 35 min at 55 °C gave hybrid **2**, eluting at t_R = 18 min. Alternatively, the hybrid was dissolved in 50 mM NH_4Ac buffer and subjected to cartridge purification (C18 column, Vac 35 cm^3), using a gradient of CH_3CN in 10 mM NH_4Ac buffer, 0–25%. Hybrid **2** eluted at 10%, yield 7 mg (3.4 μmol, 40%): MALDI-TOF-MS *m/z* calcd for $C_{77}H_{89}N_{15}O_{42}P_6$, $[M - H]^-$ 2081, *m/z* obsd 2080.

*(CG)$_8$TRPA (**3**).* The assembly of **3** used general protocol B, starting from **11** (10 mg, 12 μmol) and **8** (368 mg, 320 μmol) in pyridine and CH_3CN (2.5 mL, 4/1, v/v) for 2 h at −40 °C. HPLC purification (C18 column) used a gradient of CH_3CN in 10 mM TEAA buffer, 7–25% in 36 min at 55 °C. Hybrid **3** eluted at t_R = 18 min. Cartridge purification used a gradient of CH_3CN in 10 mM NH_4Ac buffer, 0–20%. Hybrid **3** eluted at 10% and was obtained in a yield of 50 mg (8.6 μmol, 75%): MALDI-TOF-MS *m/z* calcd for $C_{210}H_{240}N_{64}O_{104}P_{16}$, $[M - H]^-$ 5819, *m/z* obsd 5819.

*(TC)$_8$TRPA (**4**).* General protocol B was used, starting from TRPA core **11** (3.5 mg, 4 μmol) and **9** (120 mg, 114 μmol) in pyridine and CH_3CN (2.5 mL, 4/1, v/v) for 2 h at −40 °C. After complete deprotection one fraction was subjected to HPLC purification (C18 column), using a gradient of CH_3CN in 10 mM TEAA buffer, 5–25% in 40 min at 55 °C, with elution of hybrid **4** at t_R = 22 min. Cartridge purification used a gradient of CH_3CN in 10 mM NH_4Ac buffer, 0–25%. Hybrid **4** eluted at 12%, yield 6 mg (1.1 μmol, 27%): MALDI-TOF-MS *m/z* calcd for $C_{210}H_{247}N_{40}O_{112}P_{16}$, $[M - H]^-$ 5619, *m/z* obsd 5618.

*(CG)$_8$TREA (**5**).* General protocol B was employed, starting from TREA core **12** (20 mg, 20.6 μmol) and **8** (664 mg, 578 μmol) in pyridine and CH_3CN (2.5 mL, 4/1, v/v) for 2 h at −40 °C. HPLC purification (C18 column) used a gradient of CH_3CN in 10 mM TEAA buffer, 15–25% in 60 min at 55 °C. Hybrid **5** eluted at t_R = 25, 26, 27, 28, 29, and 30 min (compare Figure 4). Alternatively, the crude hybrid was dissolved in 50 mM NH_4Ac buffer and subjected to cartridge purification (C18 column, Vac 35 cm^3), using a gradient of CH_3CN in 10 mM NH_4Ac buffer, 0–20%. Hybrid **5** eluted at 12–17% and was obtained in a yield of 34 mg (5.8 μmol, 30%): MALDI-TOF-MS *m/z* calcd for $C_{218}H_{240}N_{64}O_{104}P_{16}$, $[M - H]^-$ 5915, *m/z* obsd 5913.

*(TC)$_8$TREA (**6**).* The synthesis of **6** was performed according to general protocol B, starting from TREA core **12** (5 mg, 5 μmol) and **9** (152 mg, 145 μmol, 3.5 equiv per phenolic group of core) in pyridine and CH_3CN (3.0 mL, 4/1, v/v) for 2 h at −40 °C. After complete deprotection, one portion of the crude product was dissolved in 10 mM TEAA buffer containing 7% CH_3CN and subjected to HPLC purification (C18 column, 250 × 20 mm), using a gradient of CH_3CN in 10 mM TEAA buffer, 7.5–25% in 35 min at 55 °C. Hybrid **6** eluted at t_R = 20, 21, 22, 23, 23, 24, 24, and 25 min. The remaining crude product was dissolved in 50 mM NH_4Ac buffer and subjected to cartridge purification (C18 column, Vac 35 cm^3), using a gradient of CH_3CN in 10 mM NH_4Ac buffer, 0–50%. Hybrid **6** eluted at 10–20% and was obtained in a yield of 14.4 mg (2.5 μmol, 49%): MALDI-TOF-MS *m/z* calcd for $C_{218}H_{248}N_{40}O_{112}P_{16}$, $[M - H]^-$ 5715, *m/z* obsd 5713.

■ ASSOCIATED CONTENT

Ⓢ Supporting Information

Figures, tables, and a CIF file giving a collection of NMR spectra, HPLC chromatograms, MALDI-TOF mass spectra, UV-melting data, and data on the crystal structure of **13**. This material is available free of charge via the Internet at http://pubs.acs.org.

■ AUTHOR INFORMATION

Corresponding Author

*C.R.: fax, int-49 (0) 711 608 64321; tel, int-49 (0) 711 608 64311; e-mail, lehrstuhl-2@oc.uni-stuttgart.de.

Notes

The authors declare no competing financial interest.

■ ACKNOWLEDGMENTS

The authors thank Prof. Michael Mastalerz for a gift of 2,7,14-trihydroxytriptycene, Dr. Wolfgang Frey for solving the X-ray crystal structure of **13**, Thomas Sabirov for help with the purification of **1**, Dr. Birgit Claasen for help with the acquisition of NMR spectra, and Deutsche Forschungsgemeinschaft for financial support (Grant No. RI 1063/13-1 to C.R.).

■ REFERENCES

(1) Watson, J. D.; Crick, F. H. *Nature* **1953**, *171*, 964–967.

(2) Alberts, B.; Bray, D.; Lewis, J.; Raff, M.; Roberts, K.; Watson, J. D. *The Molecular Biology of the Cell*; Garland: New York, 1983; pp 221–226.

(3) Seeman, N. C. *Nature* **2003**, *421*, 427–431.

(4) (a) Rothemund, P. W. K. *Nature* **2006**, *440*, 297–302. (b) Woo, S.; Rothemund, P. W. K. *Nat. Chem.* **2011**, *3*, 620–627.

(5) (a) Douglas, S. M.; Dietz, H.; Liedl, T.; Högberg, B.; Graf, F.; Shih, W. M. *Nature* **2009**, *459*, 414–418. (b) Dietz, H.; Douglas, S. M.; Shih, W. M. *Science* **2009**, *325*, 725–730.

(6) Said, H.; Schueller, V.; Eber, F.; Wege, C.; Liedl, T.; Richert, C. *Nanoscale* **2013**, *5*, 284–290.

(7) Alivisatos, A. P.; Johnsson, K. P.; Peng, X.; Wilson, T. E.; Loweth, C. J.; Bruchez, M. P.; Schultz, P. G. *Nature* **1996**, *382*, 609–611.

(8) Mirkin, C. A.; Letsinger, R. L.; Mucic, R. C.; Storhoff, J. J. *Nature* **1996**, *382*, 607–609.

(9) (a) Nykypanchuk, D.; Maye, M. M.; van der Lelie, D.; Gang, O. *Nature* **2008**, *451*, 549–552. (b) Park, S. Y.; Lytton-Jean, A. K. R.; Lee, B.; Weigand, S.; Schatz, G. C.; Mirkin, C. A. *Nature* **2008**, *451*, 553–556.

(10) Meng, M.; Müller, K.; Heimann, K.; Richert, C. *Small* **2008**, *4*, 1040–1042.

(11) Aldaye, F. A.; Sleiman, H. F. *Angew. Chem., Int. Ed.* **2006**, *45*, 2204–2209.

(12) Aldaye, F. A.; Palmer, A. L.; Sleiman, H. F. *Science* **2008**, *321*, 1795–1799.

(13) Stepp, B. R.; Gibbs-Davis, J. M.; Koh, D. L. F.; Nguyen, S. T. *J. Am. Chem. Soc.* **2008**, *130*, 9628–9629.

(14) Eryazici, I.; Prytkova, T. R.; Schatz, G. C.; Nguyen, S. T. *J. Am. Chem. Soc.* **2010**, *132*, 17068–17070.

(15) McLaughlin, C. K.; Hamblin, G. D.; Sleiman, H. F. *Chem. Soc. Rev.* **2011**, *40*, 5647−5656.
(16) Meng, M.; Singh, A.; Richert, C. *Small* **2009**, *5*, 2782−2783.
(17) Meng, M.; Ahlborn, C.; Bauer, M.; Plietzsch, O.; Soomro, S. A.; Singh, A.; Muller, T.; Wenzel, W.; Bräse, S.; Richert, C. *ChemBioChem* **2009**, *10*, 1335−1339.
(18) Singh, A.; Tolev, M.; Meng, M.; Klenin, K.; Plietzsch, O.; Schilling, C. I.; Muller, T.; Nieger, M.; Bräse, S.; Wenzel, W.; Richert, C. *Angew. Chem., Int. Ed.* **2011**, *50*, 3227−3231.
(19) Singh, A.; Tolev, M.; Schilling, C. I.; Bräse, S.; Griesser, H.; Richert, . *J. Org. Chem.* **2012**, *77*, 2718−2728.
(20) Griesser, H.; Tolev, M.; Singh, A.; Sabirov, T.; Gerlach, C.; Richert, C. *J. Org. Chem.* **2012**, *77*, 2703−2717.
(21) Zhang, C.; Chen, C.-F. *J. Org. Chem.* **2006**, *71*, 6626−6629.
(22) Hua, D. H.; Tamura, M.; Huang, X.; Stephany, H. A.; Helfrich, B. A.; Perchellet, E. M.; Sperfslage, B. J.; Perchellet, J.-P.; Jiang, S.; Kyle, D. E.; Chiang, P. K. *J. Org. Chem.* **2002**, *67*, 2907−2912.
(23) Yang, J.-S.; Liu, C.-P.; Lin, B. C.; Tu, C. W.; Lee, G. H. *J. Org. Chem.* **2002**, *67*, 7343−7354.
(24) Long, T. M.; Swager, T. M. *J. Am. Chem. Soc.* **2003**, *125*, 14113−14119.
(25) Newman, H. *Synthesis* **1977**, 692−693.
(26) Reichert, V.; Mathias, L. *Macromolecules* **1994**, *27*, 1030−1034.
(27) Merkushev, E. B. *Synthesis* **1980**, *6*, 486−487.